

Published in final edited form as:

Nat Neurosci. 2014 December ; 17(12): 1744–1750. doi:10.1038/nn.3861.

Leptin-inhibited PBN neurons enhance counter-regulatory responses to hypoglycemia in negative energy balance

Jonathan N. Flak^{#1}, Christa M. Patterson^{#1}, Alastair S. Garfield^{#2}, Giuseppe D'Agostino³, Paulette B. Goforth⁴, Amy K. Sutton^{1,5}, Paige A. Malec⁶, Jenny-Marie T. Wong⁶, Mark Germani¹, Justin C. Jones¹, Michael Rajala¹, Leslie Satin⁴, Christopher J. Rhodes⁷, David P. Olson⁸, Robert T. Kennedy⁶, Lora K. Heisler^{3,9}, and Martin G. Myers Jr.^{1,4,9}

¹Department of Internal Medicine, University of Michigan, Ann Arbor, MI, USA

²Center for Integrative Physiology, University of Edinburgh, Edinburgh, UK

³Rowett Institute of Nutrition and Health, University of Aberdeen, Aberdeen, and Department of Pharmacology, University of Cambridge, Cambridge, UK

⁴Department of Pharmacology, University of Michigan, Ann Arbor, MI, USA

⁵Molecular and Integrative Physiology, University of Michigan, Ann Arbor, MI, USA

⁶Department of Chemistry, University of Michigan, Ann Arbor, MI, USA

⁷Kovler Diabetes Center, University of Chicago, Chicago, IL, USA

⁸Department of Pediatrics and Communicable Diseases, University of Michigan, Ann Arbor, MI, USA

[#] These authors contributed equally to this work.

Abstract

Hypoglycemia initiates the counter regulatory response (CRR), in which the sympathetic nervous system, glucagon, and glucocorticoids restore glucose to appropriate concentrations. During starvation, low leptin restrains energy utilization, enhancing long-term survival. To ensure short-term survival during hypoglycemia in fasted animals, the CRR must overcome this energy-sparing program and nutrient depletion. Here, we identify in mice a previously unrecognized role for leptin and a population of leptin-regulated neurons that modulate the CRR to meet these challenges. Hypoglycemia activates leptin receptor (LepRb) and cholecystokinin (CCK)-expressing neurons of the parabrachial nucleus (PBN), which project to the ventromedial hypothalamic nucleus. Leptin inhibits these cells and *Cck^{cre}*-mediated ablation of LepRb enhances

Users may view, print, copy, and download text and data-mine the content in such documents, for the purposes of academic research, subject always to the full Conditions of use:http://www.nature.com/authors/editorial_policies/license.html#terms

⁹Correspondence: Martin G Myers, Jr., MD, PhD, Departments of Internal Medicine and Molecular and Integrative Physiology, University of Michigan, 1000 Wall St; 6317 Brehm Tower, Ann Arbor, MI 48105, Phone: 734-647-9515, Fax: 734-232-8175, mgyers@umich.edu; Lora K. Heisler, PhD, Rowett Institute of Nutrition and Health, University of Aberdeen, Aberdeen, UK AB21 9SB, Tel: 01224 437446, Fax: 01224 437300, lora.heisler@abdn.ac.uk.

Author contributions: JNF and CMP produced the data in Figs. 1-5 and Supplemental Figs. 1-10, with the exception of the data in Figures 1e-I (produced by PBG and LS) and measurements of catecholamines, which were performed by PM, J-MTW and RTK. MG and MR helped produce Supplemental Figs 2, 5, and 10. JCJ aided with Figures 2-4 and with animal genotyping and husbandry. GD'A, ASG, and LKH performed the experiments in Fig. 6. Adenoviral tracers were produced by AKS and CJR. Experimental design, interpretation, and manuscript preparation were led by MGM, LKH, JNF, CMP, ASG and DPO.

the CRR. Inhibition of PBN LepRb cells blunts the CRR, while their activation mimics the CRR in a CCK-dependent manner. PBN LepRb^{CCK} neurons represent a crucial component of the CRR system, and may represent a therapeutic target in hypoglycemia.

Hypoglycemia and glucoprivation (which mimics low glucose availability by interfering with cellular glucose metabolism) activate a neurohormonal counter-regulatory response (CRR) that stimulates the hypothalamic-pituitary-adrenal (HPA) axis and the sympathetic nervous system (SNS) to promote glucose release into the bloodstream^{1,2}. The SNS also acts on pancreatic islets to promote glucagon release and suppress insulin secretion³. The CRR serves to restore normoglycemia and protect the brain/body from damage due to hypoglycemia. An appropriately robust CRR is crucial to prevent cognitive impairment, unconsciousness, or even death when blood glucose levels fall too low. This response is especially crucial to counteract insulin-induced hypoglycemia (IIH) in diabetic patients, for whom the risk of hypoglycemia (especially during the night and other periods of fasting) represents the most serious limitation to achieving tight glycemic control^{2,4}. Defining the neural systems that mediate and modulate the CRR to hypoglycemia will reveal mechanisms that represent potential targets for the prevention and therapy of this life-threatening complication of insulin therapy.

Diminished nutritional reserves present a particularly severe challenge to mounting an appropriate CRR to hypoglycemia; not only does fasting predispose to hypoglycemia⁵ and deplete stores of glycogen and gluconeogenic substrates, but also negative energy balance initiates a neuroendocrine starvation response—decreasing overall SNS tone and initiating energy-sparing changes in endocrine function⁶. Teleologically, it would thus make sense to deploy a more robust CRR in the face of depleted energy stores, although such a system has not been described previously.

The energy-conserving response to starvation results in large part from decreased circulating concentrations of the adipose-derived hormone leptin, which is produced in proportion to fat stores⁶⁻⁹. In general, low leptin signals the insufficiency of energy reserves to decrease energy utilization and promote hunger, along with other adaptations to cope with decreased energy availability, including alterations in anxiety, motivation, locomotor activity, glucose homeostasis and a wide range of other behavioral and physiologic parameters¹⁰⁻¹⁴. Here, we test the hypothesis that low leptin also enhances the CRR to permit an appropriately robust response to hypoglycemia in the context of decreased nutritional reserves.

Results

Glucose- and leptin-inhibited PBN LepRb neurons project to the VMH

Most leptin effects are mediated via LepRb in the brain, especially the hypothalamus and brainstem, where most LepRb neurons reside¹⁵⁻¹⁷. Commensurate with the diverse processes controlled by leptin, various subtypes of LepRb neurons each contribute to distinct aspects of energy balance and metabolism^{13,18-20}. Hypothalamic LepRb neurons in aggregate mediate most of leptin's action on food intake and energy expenditure²¹⁻²³. Although ablation of LepRb in the nucleus tractus solitarius (NTS) has revealed that NTS

LepRb cells participate in the control of satiety²⁴⁻²⁸, roles for leptin/LepRb in most brainstem sites remain essentially unstudied. Genetic markers such as enhanced yellow fluorescent protein (eYFP) in *Lepr^{cre};Rosa26-eYFP* (LepRb^{eYFP}) mice, along with the leptin-induced phosphorylation of STAT3 (pSTAT3; a marker of LepRb activity), reveal that the brainstem parabrachial nucleus (PBN) contains a substantial number of LepRb neurons (Fig. 1a and Supplemental Fig. 1)^{13,18-20}.

To understand potential functions for PBN LepRb neurons, we examined their projections by injecting Ad-iN/Syn-mCherry²⁹ into the PBN of LepRb^{eYFP} animals to reveal the location(s) of synaptic terminals from PBN LepRb cells by the presence of mCherry-immunoreactivity (-IR) (Fig. 1a-c). This analysis revealed that synaptic terminals from PBN LepRb neurons primarily target the dorsomedial compartment of the ventromedial hypothalamic nucleus (dmVMH; a site important for SNS function, including the CRR to hypoglycemia³⁰⁻³⁴).

Since PBN LepRb neurons target the dmVMH, we postulated that PBN LepRb neurons might respond to hypoglycemia or glucoprivation. Indeed, IIH and 2-deoxyglucose (2DG; which inhibits glucose metabolism to mimic cellular hypoglycemia)-induced glucoprivation both promoted cFos-IR (a histochemical marker that often reflects increased neuronal activity) in many PBN LepRb neurons (Supplemental Fig. 2). The distributions of IIH- and 2DG-induced cFos-IR in the PBN LepRb neurons were similar, suggesting similar actions on these neurons by the two stimuli (Supplemental Fig. 3). Furthermore, decreased glucose concentrations depolarized and increased the firing frequency of approximately half (6/11) of the examined PBN LepRb neurons in electrophysiological slice preparations (Fig. 1d-f). Conversely, leptin hyperpolarized and decreased the firing rate of PBN LepRb neurons in low glucose (Fig. 1g-i).

Together, the projection of hypoglycemia-activated, leptin-inhibited PBN LepRb neurons to the VMH suggests that these cells might participate in the CRR to glucoprivation, while the withdrawal of leptin-mediated inhibition from PBN LepRb neurons might enhance the CRR in low-leptin states. Such a system could serve to overcome the limitations imposed by starvation, enabling an appropriate CRR in spite of decreased energy stores and baseline SNS tone. Indeed, leptin and energy balance modulate the amplitude of the CRR: a 12-hour fast exaggerates the CRR to 2DG in mice, while exogenous leptin blunts this fasting-induced augmentation of the CRR (Supplemental Fig. 4). Hence, the fall in leptin during negative energy balance enhances the acute response to glucoprivation (thereby counteracting the inadequate CRR that might otherwise result).

Exaggerated CRR in mice lacking LepRb from PBN LepRb^{CCK} neurons

To understand whether PBN LepRb neurons might enhance the CRR in low-leptin states, we sought a molecular marker to permit the manipulation of PBN LepRb neurons. Since cholecystinin (CCK)-containing PBN neurons project to the VMH^{35,36}, we examined the potential expression of LepRb in PBN CCK neurons. We bred *Cck^{cre}* mice to the *ROSA26-eYFP* background to generate CCK^{eYFP} mice and examined the induction of pSTAT3-IR in CCK^{eYFP} cells, demonstrating that many PBN LepRb cells express CCK (LepRb^{CCK} neurons) (Fig. 2a, b). While some LepRb^{CCK} cells were also observed in other brainstem

regions (including the Edinger-Westphal (EW), periaqueductal grey (PAG), and NTS) (data not shown), LepRb^{CCK} neurons were absent from the hypothalamus and other brain areas. As for PBN LepRb neurons, we observed increased cFos-IR in PBN CCK cells following treatment with 2DG (Supplemental Fig. 5), suggesting that PBN LepRb^{CCK} cells represent the subpopulation of PBN LepRb cells that are activated by glucoprivation.

To understand the function of these brainstem LepRb^{CCK} cells in leptin action, we crossed *Cck^{cre}* onto the *Lep^{fllox}* background to generate mice lacking LepRb expression specifically in LepRb^{CCK} neurons (*LepRb^{Cck}KO* animals) (Fig. 2a). As expected, leptin-stimulated pSTAT3-IR was absent from CCK-expressing PBN neurons in *LepRb^{Cck}KO* mice, and overall leptin-stimulated PBN pSTAT3-IR was reduced by approximately 75% in the PBN of *LepRb^{Cck}KO* animals compared to controls (Fig. 2b, c). Leptin-stimulated pSTAT3-IR was also significantly reduced in the EW, but not in other brain areas (Supplemental Fig. 6). Thus, *Cck^{cre}* ablates LepRb expression in the LepRb^{CCK} cells of the brainstem PBN and EW nuclei.

We detected no alteration in body weight, endocrine function, glucose homeostasis or glucose tolerance in *LepRb^{Cck}KO* mice compared to controls (Supplemental Fig. 7). Consistent with an enhanced CRR, however, *LepRb^{Cck}KO* mice displayed blunted IIH (Fig. 2d). Indeed, like fasted mice (Supplemental Figure 3), *LepRb^{Cck}KO* mice exhibited more robust glycemic excursions in response to 2DG than did controls (Fig. 2e). Furthermore, while insulin was unchanged (data not shown), circulating glucagon, corticosterone and epinephrine concentrations were increased in *LepRb^{Cck}KO* mice compared to controls 90 minutes after 2DG administration (Fig. 2f-h). The increased glycemic excursion in response to glucoprivation exhibited by *LepRb^{Cck}KO* mice is similar to that observed in fasted control animals, and even prolonged fasting fails to further enhance this response in *LepRb^{Cck}KO* mice, suggesting overlapping mechanisms for leptin action on LepRb^{CCK} neurons and the augmented CRR observed with prolonged fasting (Supplemental Fig. 8). Furthermore, these cells are at least partly specific to hypoglycemia (as opposed to all stressors), since restraint stress provoked no increase in cFos in PBN LepRb neurons, and the hyperglycemic response to restraint stress was normal in *LepRb^{Cck}KO* mice (Supplemental Fig. 9).

To examine IIH directly, we subjected the *LepRb^{Cck}KO* mice to hypoglycemic clamp analysis, in which high levels of insulin are continuously infused while the glucose infusion rate is varied to maintain the desired level of hypoglycemia, thereby examining counter-regulatory glucose production during IIH (Fig. 3). The glucose infusion rate required to prevent blood glucose from falling below the clamped level was decreased in *LepRb^{Cck}KO* mice compared to controls, consistent with increased counter-regulatory hepatic glucose production in these animals (Fig. 3a-c). Indeed, the hepatic expression of *glucose-6-phosphatase* (*G6Pase*, which dephosphorylates glucose to permit its efflux from the cell) was increased in *LepRb^{Cck}KO* mice compared to controls at the end of the clamp (Fig. 3d). Note that *G6Pase* expression, which is decreased by insulin, is augmented by counter-regulatory stimuli that increase cAMP, including epinephrine and glucagon³⁷, and thereby provides an indirect indication of the liver's potential to release glucose. Thus, leptin action via LepRb^{CCK} neurons does not contribute to baseline glucose tolerance, but rather

enhances the CRR by promoting increased counter-regulatory hormone release and hepatic glucose output.

DREADD-mediated inhibition of PBN LepRb neurons blunts the CRR

To evaluate the function of PBN LepRb neurons, specifically, we utilized the stereotaxic injection of AAVs that mediate the cre-dependent expression of designer receptors exclusively activated by designer drugs (DREADDs; expressed as DREADD-mCherry fusion proteins). DREADDs are genetically-engineered muscarinic receptor variants that are insensitive to endogenous ligands, but which are activated by the otherwise biologically inert clozapine-N-oxide (CNO)^{38,39}; CNO activates neurons containing the G_q-coupled hM3D_q and inhibits neurons that contain the G_i-coupled hM4D_i^{38,39}.

To determine the role for PBN LepRb neurons in the endogenous CRR, we injected the inhibitory AAV-hM4D_i bilaterally into the PBN of *Lep^{rcre}* animals, allowed the animals to recover for several weeks, and examined the response to 2DG-mediated glucoprivation in the presence or absence of CNO (Fig. 4a-c). We found that CNO significantly blunted the increase in blood glucose concentrations following 2DG treatment in mice that expressed hM4D_i in PBN LepRb neurons. Thus, inhibition of PBN LepRb cells impairs the CRR, demonstrating that PBN LepRb neurons play an integral role in the response to glucoprivation.

DREADD-mediated activation of PBN LepRb neurons mimics the CRR

Our findings predict that activation of PBN LepRb neurons should mimic the CRR. To test this, we injected the activating AAV-hM3D_q bilaterally into the PBN of *Lep^{rcre}* animals and, following a several-week recovery period, treated them with CNO (Fig. 5). CNO treatment increased cFos-IR in the PBN and the VMH of these animals compared to vehicle (Supplemental Fig. 10), as would be expected upon activation of the PBN LepRb→VMH circuit. CNO also increased blood glucose concentrations (Fig. 5b, c), along with glucagon and corticosterone, while tending to decrease insulin compared to vehicle (Fig. 5d-f). Since the effect of increased glucose on pancreatic islets would cause glucagon to fall and insulin to rise, the opposite finding (that glucagon rose while insulin tended to fall) implies increased SNS outflow to the pancreatic islets upon activation of PBN LepRb cells. Activation of PBN LepRb neurons also increased hepatic *G6Pase* expression (Fig. 5g). Thus, activation of PBN LepRb neurons increases circulating concentrations of counter-regulatory hormones and hepatic glucose production to raise blood glucose, similar to the native CRR.

Role for CCK in the function of PBN LepRb neurons

To determine the role for CCK in the PBN LepRb neuron-mediated stimulation of blood glucose, we injected AAV-hM3D_q virus bilaterally into the PBN of *Lep^{rcre}* animals, allowed them to recover for several weeks, and treated them with CNO in the presence or absence of the CCK receptor inhibitor, proglumide (Fig. 6a, b). Pretreatment with proglumide blocked the increase in blood glucose and hepatic *G6pase* expression during CNO-mediated activation of PBN LepRb neurons. This requirement for CCK signaling in the hyperglycemic response to activated PBN LepRb neurons suggests that the LepRb^{CCK}

subpopulation of PBN LepRb neurons mediates this response, consistent with the exaggerated CRR displayed by the *LepRb^{Cck}KO* mice. To determine whether CCK is also required for the normal response to glucoprivation, we also examined the effect of proglumide on the hyperglycemic response to 2DG in normal C57Bl/6 mice (Fig. 6c). While proglumide did not lower baseline blood glucose, it blunted the response to 2DG (similar to the DREADD hM4D_i-mediated inhibition of PBN LepRb neurons), revealing the importance of CCK neurotransmission for the endogenous response to glucoprivation.

Discussion

Our findings reveal that low leptin enhances the CRR, identify a previously unknown component of the neural circuitry that mediates the CRR (along with the neuropeptide (CCK) by which it acts, and demonstrate that leptin action via these cells to modulate the CRR (Supplemental Fig. 11).

We report that low glucose activates PBN LepRb cells in electrophysiologic slice preparations. These data suggest that PBN LepRb neurons either sense low glucose directly or receive inputs from other glucose-sensing cells within the slice preparations. It is also possible that PBN LepRb cells receive additional input from other PBN projecting neurons that sense hypoglycemia. Furthermore, neurons that convey information relevant to other physiologic emergencies that demand an appropriately robust response, even when energy stores are depleted, might also activate these neurons to promote the CRR and permit its enhancement by low leptin. Gut peptides, such as amylin, that activate the NTS→PBN→CeA anorexia circuit⁴⁰ do not activate PBN LepRb neurons, however (data not shown). Furthermore, restraint stress fails to activate PBN LepRb neurons by the criterion of cFos accumulation, and the hyperglycemic response to restraint is normal in *LepRb^{Cck}KO* mice, suggesting some specificity of PBN LepRb neurons for the CRR to hypoglycemia.

Leptin inhibits PBN LepRb neurons in electrophysiologic slice preparations, suggesting that decreased leptin action on PBN LepRb neurons would augment the CRR. Indeed, deletion of LepRb from the LepRb^{CCK} cells (approximately 75% of PBN LepRb neurons) enhances the CRR without altering energy balance or other parameters of glucose homeostasis. Thus, our findings reveal a mechanism by which low leptin can enhance the allostatic response to acute hypoglycemia (as required in the face of depleted energy stores and decreased baseline SNS tone), without altering baseline energy and glucose homeostasis. Like the attenuation of overall energy expenditure during caloric restriction⁶, diminished leptin action underlies the enhanced CRR in fasted animals. Thus, low leptin enhances the CRR, in addition to increasing appetite and blunting baseline energy expenditure. Hence, not only do these findings reveal a previously unrecognized neural system that regulates the CRR, but they also demonstrate a broader and previously undescribed role for (low) leptin in adapting allostatic physiology appropriately for limited nutritional reserves. Fasting increases the risk for hypoglycemia⁵, and this system presumably ensures the adequacy of the response to hypoglycemia under these conditions. Importantly, since the PBN LepRb neurons do not alter baseline glucose homeostasis, but rather enhances the CRR during hypoglycemia,

agents that sensitize these cells could be therapeutically useful to mitigate hypoglycemia while not disrupting tight glycemic control.

Low glucose or glucoprivic stimuli activate PBN LepRb cells that project to the dmVMH. The pharmacogenetic activation of these cells promotes cFos in the dmVMH and mimics the CRR in a CCK-dependent manner-increasing blood glucose, counter-regulatory hormones, and markers of hepatic glucose production. Furthermore, pharmacogenetic inhibition of PBN LepRb neurons blunts the response to glucoprivation (as does inhibition of CCK signaling), demonstrating the role for PBN LepRb^{CCK} neurons in the normal glucoprivic response. The CCK-responsive cells that lie downstream of the PBN LepRb neurons presumably represent crucial effectors of the CRR, and it will be important to identify these neurons and understand their function. Our identification of a discrete neural system that mediates and modulates the CRR provides a potential target for therapeutic intervention to mitigate iatrogenic IHH and improve the safety and efficacy of insulin therapy in diabetes mellitus.

Materials and Methods

Animals

All of the procedures listed in this manuscript were approved by the University of Michigan Committee on the Use and Care of Animals or were in accordance with the U.K. Animals (Scientific Procedures) Act 1986. C57Bl/6J males were from Jackson Laboratories. *Lep^{rcre}* mice on the C57Bl/6 background have been described¹⁹ and were bred in our colony. *CCK^{tm1.1(cre)Zjh}* mice were purchased from Jackson laboratories and crossed to *Lep^{rfllox}* or *Rosa26^{eYFP}* mice from our colony^{41,42}. *LepRb^{CckKO}* study animals (along with *Cck^{cre}*, *Lep^{rfllox/fllox}*, and wild-type controls) were generated in our colony by crossing *Cck^{cre};Lep^{rfllox/+}* and *Lep^{rfllox/+}* animals; these animals were on the segregating C57Bl/6;129Sv background. Mice were kept in a temperature-controlled room on a 12:12 light dark cycle and provided with *ad libitum* food and water unless otherwise noted. Data reported are from single housed male animals studied during the light cycle, except for neuroanatomic studies, which were carried out in group housed mixed male and female mice. For studies, animals were processed in the order of their ear tag number, which was randomly assigned at the time of tailing (prior to genotyping). Investigators were blinded to genotype/treatment for all studies except DREADD activation experiments.

Electrophysiologic studies

3-5 week old LepRb reporter mice of either sex were euthanized by decapitation. Horizontal slices (250 μ M) were prepared in oxygenated ice-cold sucrose solution containing (in mM): 220 sucrose, 2.5 KCl, 26 NaHCO₃, 1.25 NaH₂PO₄, 5 glucose, 6 MgCl₂, 1 CaCl₂ using a VT 1200S vibratome (Leica Microsystems Inc., Buffalo Grove, IL). Slices were allowed to recover for at least 1 hr before electrophysiological analysis in a holding chamber containing oxygenated artificial cerebrospinal fluid (aCSF) solution containing (in mM): 125 NaCl, 3 KCl, 1.25 NaH₂PO₄, NaHCO₃, 2 glucose, 1 MgCl₂, 2.5 CaCl₂, pH 7.4. Individual fluorescently labeled IPBN LepRb neurons were visualized using an Olympus BX51WI upright microscope equipped with IR-DIC optics (Olympus, Tokyo, Japan). Patch electrodes

made from borosilicate glass capillaries (Warner Instruments, Hamden, CT) were pulled to a tip resistance of 3-7 M Ω using a Brown/Flaming P-97 micropipette puller (Sutter Instr. Co., Novato, CA) and filled with a solution containing (in mM): 130 K gluconate, 10 KCl, 1 EGTA, 10 HEPES, 0.6 NaGTP, 2 MgATP, 8 phosphocreatine, pH 7.2. Slices were perfused with aCSF solution warmed to 32-33° C using a TC-344 temperature controller and preheater (Warner Instruments, Hamden, CT) and continuously bubbled with 5% CO₂ and 95% O₂. Low glucose aCSF (0.5 mM, osmolarity adjusted with sucrose) and leptin were applied via bath perfusion. Membrane potentials were measured using an Axopatch 200B amplifier (Molecular Devices, Sunnyvale, CA) in tight-seal whole-cell current clamp mode. Currents were filtered at 5 kHz, digitized at 10 kHz and analyzed offline. Data were not corrected for a junction potential 14.7 mV. Neurons selected for analysis had stable series resistances (Rs) < 25 M Ω that were not compensated.

Phenotypic Studies

Starting at 21 days of age, animals were singly housed. Blood glucose and body weight were monitored weekly in these animals starting at 28 days. Beginning at 10 weeks of age, glucose homeostasis was examined by glucose tolerance test (GTT; 2 g/kg, IP), insulin tolerance test (ITT; 1.2 units/kg Humulin (Eli Lilly), IP) and 2DG (Sigma) challenge (250 or 500 mg/kg, IP). The animals were allowed at least 10 days of recovery prior to each challenge. Mice were fasted for four hours prior to each challenge: Food was removed following lights on and testing followed four hours later. Tail vein blood was collected for the measurement of glucose (one touch ultra 2 glucometer (Johnson and Johnson)). Plasma or serum was prepared from larger volume samples and stored at -20°C for later assay. Samples for the determination of epinephrine concentrations were obtained from animals with an arterial catheter (placed by the UM Animal Phenotyping Core (APC)). Glucagon (Millipore) and Glucocorticoid (MP Biomedicals) levels were determined via radioimmunoassay, while insulin and leptin were determined via multiplex assay (Millipore).

Determination of plasma epinephrine concentrations

Five μ L of plasma was spiked with 1.25 μ L of D6-epinephrine as an internal standard. Proteins were removed by addition of 25 μ L of ice cold acetonitrile, followed by centrifugation for 10 min at 13,400 rpm. Twenty μ L of the supernatant was removed and benzoylated⁴³ by sequential addition of 10 μ L of 100 mM sodium tetraborate, 10 μ L of benzoyl chloride (2% in acetonitrile, v/v), and 10 μ L of sulfuric acid (1% in DMSO, v/v). Standard solutions of epinephrine were prepared in aCSF, which is similar in composition to plasma without protein⁴⁴, to create a calibration range of 0.1 – 20 nM. Standards were spiked with internal standard, diluted with acetonitrile, and derivatized as above. Calibration curves were prepared based on the peak area ratio of the standard to the internal standard by linear regression. All samples and standards were analyzed in triplicate using an Acquity HSS T3 C18 chromatography column (1 mm \times 100 mm, 1.8 μ m, 100 Å pore size) in a nanoAcquity UPLC (Waters) interfaced to an Agilent 6410 triple quadrupole mass spectrometer. Mobile phase A was 10 mM ammonium formate with 0.15% (v/v) formic acid in water. Mobile phase B was acetonitrile. The gradient used was: initial, 0% B; 0.01 min, 23% B; 2.51 min, 23% B, 3 min, 50% B; 5.3 min, 60% B; 6.46 min, 65% B; 6.47 min,

100% B; 7.49 min, 100% B; 7.5 min, 0% B; 8.5 min, 0% B at 100 μ L/min. Benzoylated epinephrine eluted at 6.85 min. The sample injection volume was 5 μ L in partial loop injection mode. The autosampler was kept at ambient temperature and the column was held at 27 $^{\circ}$ C. Electrospray ionization was used in positive mode at 4 kV. The gas temperature was 350 $^{\circ}$ C, gas flow was 11 L/min, and the nebulizer was at 15 psi. Ions were detected in MS-MS mode with precursor ions of 496 and 502 m/z for benzoylated epinephrine and D6-epinephrine, respectively, and product ion 105 m/z for both. The following voltage settings were used: fragmentor = 120 V, collision energy = 15 V, and cell accelerator = 4 V. Automated peak integration was performed using Agilent MassHunter Workstation Quantitative Analysis for QQQ, version B.05.00. All peaks were visually inspected to ensure proper integration.

Hyperinsulinemic-hypoglycemic Clamp

Following a 5-hour fast, the UM APC infused conscious, unstressed, catheterized mice with 10mU/kg/min insulin and glucose was clamped at \sim 50mg/dl for 120 minutes by the infusion of glucose^{45,46}. Following hyperinsulinemic-hypoglycemic clamp, animals were euthanized for the collection of liver and brain tissue.

Perfusion and Immunohistochemistry

Where indicated, mice were treated with leptin (5mg/kg; the generous gift of AstraZeneca Pharmaceuticals) 2 hours prior to perfusion to label leptin-responsive neurons via the induction of pSTAT3-IR. The mice were anesthetized with sodium pentobarbital and a lobe of liver removed prior to transcardial perfusion and collection of the brain. The brains were sectioned coronally at 30 μ m on a freezing microtome and distributed into 4 series for analysis. Series were pre-treated with 1% Hydrogen Peroxide followed by individual washes of PBS with 0.3% Glycine and 0.03% SDS. The sections were incubated overnight at room temperature in the rabbit anti-cFos (Santa Cruz, sc-52; 1:1000), chicken anti-GFP (Abcam, ab12970; 1:1000), rabbit anti-dsred (living colors, 632496; 1:1000), and/or rabbit anti-pSTAT3 (Cell Signaling Technology, 91455; 1:500) antibody and exposed the next day with either biotinylated (1:200 followed by ABC amplification and DAB reaction) or fluorescent secondary antibody (Molecular Probes, 1:200) in order to visualize proteins. Each of these antibodies is included on the Journal of Comparative Neurology Antibody database (http://onlinelibrary.wiley.com/journal/10.1002/%28ISSN%291096-9861/homepage/jcn_antibody_database.htm). The sections were mounted on glass slides and coverslipped with vectashield mounting media (Vector labs) for later image capture. Images were collected on an Olympus BX-51 microscope, and immunoreactive cells/co-labeled cells were counted manually using Adobe Photoshop. Total eYFP-IR cells were counted within the area, as well as colocalized eYFP-IR cells with nuclear marker (cFos-IR or pstat3). Cells were counted bilaterally and expressed as raw counts from each 1:4 series.

mRNA analyses

mRNA was extracted from liver samples using trizol (Invitrogen); 1 μ g was converted to complementary DNA (cDNA) using superscript reverse transcriptase kit (Invitrogen). Using the cDNA, GAPDH and target genes were analyzed via Taqman kits (Applied Biosystems)

on an Applied Biosystems 7500 Real Time PCR system. Relative mRNA expression was calculated using the 2^{-Ct} method.

Stereotaxic injection of viral constructs

Following the induction of isoflurane anesthesia and placement in a stereotaxic frame, the skulls of adult *Lepr^{Cre}* mice were exposed. After Bregma and Lambda were leveled, a guide cannula with injector was lowered into the approximate PBN coordinates from Bregma (anteroposterior: -3.3, mediolateral: 1.2, dorsoventral: -4.85). 100 nl of either Ad-iN Syn-mCherry²⁹, AAV-hM4D_i, or AAV-hM3D_q (University of North Carolina Vector Core) were injected using a 500 nl Hamilton Syringe at a rate of 20nl/minute. After 5 minutes of time post-injection for adequate dispersal and absorption of the virus, the injector and cannula were removed from the animal; the incision site was closed and sutured. The mice received pre-surgical and post-surgical analgesics. The mice injected with Ad-iN Syn-mCherry were allowed one week to recover before being sacrificed, while AAV-hM3D_q/hM4D_i were allowed at least two weeks to recover from surgery before experimentation.

Proglumide Treatment

Lepr^{Cre} mice were pretreated with AAV-hM3D_q bilaterally injected into the PBN (as described above) and at least two weeks later, were food deprived from 9:00 am to 1:00 pm, at which time the study commenced. Baseline blood glucose was determined and mice were pre-treated with 20 mg/kg of the pan-specific CCK-receptor antagonist proglumide sodium salt (Tocris Biosciences) or 0.9% sterile saline. After 30 min blood glucose was assessed and mice were administered 0.3 mg/kg CNO or 0.9% sterile saline. Blood glucose was monitored for a further 120 min. The study was repeated in C57BL/6 mice pretreated with 100 mg/kg proglumide followed by treatment with 500 mg/kg 2DG or 0.9% sterile saline 30 min later. Blood glucose was monitored for a further 180 min.

Statistics

No statistical methods were used to predetermine sample sized, but our sample sizes are similar to those reported in previous publication from our group²³. Sample sizes for experiments with stereotaxic injections of AAVs were doubled, with the prediction of a 50-60% bilateral hit rate of the PBN. The data presented includes many groups of animals and therefore do not have the same n for each experiment. Blood Glucose data over multiple time points was analyzed by two way repeated measures ANOVA with Fisher LSD post hoc test. Area under the curve (two-sided) and hormone data (one-sided) were analyzed by Student's T-test; area under the curve data in the fasting 2DG challenge experiment was analyzed by one way ANOVA with Fisher LSD Post Hoc Test. No animals were removed from analysis unless there was evidence of either sickness or injury (loss of >10% body weight or malaise). Data that did not fall in a normal distribution or equal variance was log transformed and then re-analyzed. Variance was similar among all groups. Data was deemed significant when $p < 0.05$. All statistics were performed with sigmastat (Systat).

Supplementary Material

Refer to Web version on PubMed Central for supplementary material.

Acknowledgements

We thank AstraZeneca Pharmaceuticals (San Diego, CA) for the generous gift of leptin, Dr. Bryan Roth (University of North Carolina, Chapel Hill, NC) for CNO, and members of the Myers and Heisler labs for helpful discussions. Research support was provided by the Animal Phenotyping Core of the Michigan Diabetes Research Center (NIH Grant P30 DK020572) and the Michigan Nutrition and Obesity Research Center (P30 DK089503), the American Diabetes Association, the American Heart Association and the Marilyn H. Vincent Foundation and the NIH (DK098853) to MGM, NIH DK055267 & DK020595 to CJR, NIH DK046060 (RTK), NIH DK046409 (LS), and the Wellcome Trust (098012) and BBSRC (BB/K001418/1) to LKH.

References

1. Levin BE, Dunn-Meynell AA, Routh VH. CNS sensing and regulation of peripheral glucose levels. *Int.Rev.Neurobiol.* 2002; 51:219–258. [PubMed: 12420361]
2. McCrimmon RJ, Sherwin RS. Hypoglycemia in type 1 diabetes. *Diabetes.* 2010; 59:2333–2339. [PubMed: 20876723]
3. Taborsky GJ Jr. Islets have a lot of nerve! Or do they? *Cell Metab.* 2011; 14:5–6. [PubMed: 21723498]
4. Sanders NM, et al. Feeding and neuroendocrine responses after recurrent insulin-induced hypoglycemia. *Physiol Behav.* 2006; 87:700–706. [PubMed: 16492385]
5. Awoniyi O, Rehman R, Dagogo-Jack S. Hypoglycemia in patients with type 1 diabetes: epidemiology, pathogenesis, and prevention. *Current diabetes reports.* 2013; 13:669–678. [PubMed: 23912765]
6. Ahima RS, et al. Role of leptin in the neuroendocrine response to fasting. *Nature.* 1996; 382:250–252. [PubMed: 8717038]
7. Montague CT, et al. Congenital leptin deficiency is associated with severe early onset obesity in humans. *Nature.* 1997; 387:903–908. [PubMed: 9202122]
8. Farooqi IS, et al. Effects of recombinant leptin therapy in a child with congenital leptin deficiency. *N.Engl.J.Med.* 1999; 341:879–884. [PubMed: 10486419]
9. Legrady G, Emerson CH, Ahima RS, Flier JS, Lechan RM. Leptin prevents fasting-induced suppression of prothyrotropin-releasing hormone messenger ribonucleic acid in neurons of the hypothalamic paraventricular nucleus. *Endocrinology.* 1997; 138:2569–2576. [PubMed: 9165050]
10. Gautron L, Elmquist JK. Sixteen years and counting: an update on leptin in energy balance. *The Journal of clinical investigation.* 2011; 121:2087–2093. [PubMed: 21633176]
11. Ahima RS, Saper CB, Flier JS, Elmquist JK. Leptin regulation of neuroendocrine systems. *Front Neuroendocrinol.* 2000; 21:263–307. [PubMed: 10882542]
12. Morton GJ, Cummings DE, Baskin DG, Barsh GS, Schwartz MW. Central nervous system control of food intake and body weight. *Nature.* 2006; 443:289–295. [PubMed: 16988703]
13. Myers MG Jr, Munzberg H, Leininger GM, Leshan RL. The geometry of leptin action in the brain: more complicated than a simple ARC. *Cell Metab.* 2009; 9:117–123. [PubMed: 19187770]
14. Friedman JM. Leptin at 14 y of age: an ongoing story. *Am J Clin Nutr.* 2009; 89:973S–979S. [PubMed: 19190071]
15. McMinn JE, et al. Neuronal deletion of *Lepr* elicits diabetes in mice without affecting cold tolerance or fertility. *Am.J Physiol Endocrinol.Metab.* 2005; 289:E403–E411. [PubMed: 15870101]
16. de Luca C, et al. Complete rescue of obesity, diabetes, and infertility in db/db mice by neuron-specific *LEPR-B* transgenes. *J Clin.Invest.* 2005; 115:3484–3493. [PubMed: 16284652]
17. Cohen P, et al. Selective deletion of leptin receptor in neurons leads to obesity. *The Journal of clinical investigation.* 2001; 108:1113–1121. [PubMed: 11602618]
18. Scott MM, et al. Leptin targets in the mouse brain. *J Comp Neurol.* 2009; 514:518–532. [PubMed: 19350671]
19. Patterson CM, Leshan RL, Jones JC, Myers MG Jr. Molecular mapping of mouse brain regions innervated by leptin receptor-expressing cells. *Brain Res.* 2011

20. Grill HJ. Distributed neural control of energy balance: contributions from hindbrain and hypothalamus. *Obesity*. 2006; 14(Suppl 5):216S–221S. [PubMed: 17021370]
21. Ring LE, Zeltser LM. Disruption of hypothalamic leptin signaling in mice leads to early-onset obesity, but physiological adaptations in mature animals stabilize adiposity levels. *The Journal of clinical investigation*. 2010; 120:2931–2941. [PubMed: 20592471]
22. Vong L, et al. Leptin Action on GABAergic Neurons Prevents Obesity and Reduces Inhibitory Tone to POMC Neurons. *Neuron*. 2011; 71:142–154. [PubMed: 21745644]
23. Leshan RL, Greenwald-Yarnell M, Patterson CM, Gonzalez IE, Myers MG Jr. Leptin action through hypothalamic nitric oxide synthase-1-expressing neurons controls energy balance. *Nat Med*. 2012
24. Hayes MR, et al. Endogenous leptin signaling in the caudal nucleus tractus solitarius and area postrema is required for energy balance regulation. *Cell Metab*. 2010; 11:77–83. [PubMed: 20074530]
25. Scott MM, Williams KW, Rossi J, Lee CE, Elmquist JK. Leptin receptor expression in hindbrain Glp-1 neurons regulates food intake and energy balance in mice. *The Journal of clinical investigation*. 2011; 121:2413–2421. [PubMed: 21606595]
26. Huo L, Gamber KM, Grill HJ, Bjorbaek C. Divergent leptin signaling in proglucagon neurons of the nucleus of the solitary tract in mice and rats. *Endocrinology*. 2008; 149:492–497. [PubMed: 17974623]
27. Huo L, Maeng L, Bjorbaek C, Grill HJ. Leptin and the Control of Food Intake: Neurons in the Nucleus of the Solitary Tract Are Activated by Both Gastric Distension and Leptin. *Endocrinology*. 2007; 148:2189–2197. [PubMed: 17317774]
28. Garfield AS, et al. Neurochemical characterization of body weight-regulating leptin receptor neurons in the nucleus of the solitary tract. *Endocrinology*. 2012; 153:4600–4607. [PubMed: 22869346]
29. Opland D, et al. Loss of neurotensin receptor-1 disrupts the control of the mesolimbic dopamine system by leptin and promotes hedonic feeding and obesity. *Mol Metab*. 2013; 2:423–434. [PubMed: 24327958]
30. Levin BE, Magnan C, Dunn-Meynell A, Le Foll C. Metabolic sensing and the brain: who, what, where, and how? *Endocrinology*. 2011; 152:2552–2557. [PubMed: 21521751]
31. Levin BE, Becker TC, Eiki J, Zhang BB, Dunn-Meynell AA. Ventromedial hypothalamic glucokinase is an important mediator of the counterregulatory response to insulin-induced hypoglycemia. *Diabetes*. 2008; 57:1371–1379. [PubMed: 18292346]
32. Chan O, et al. Increased GABAergic tone in the ventromedial hypothalamus contributes to suppression of counterregulatory responses after antecedent hypoglycemia. *Diabetes*. 2008; 57:1363–1370. [PubMed: 18375441]
33. Barnes MB, Lawson MA, Beverly JL. Rate of fall in blood glucose and recurrent hypoglycemia affect glucose dynamics and noradrenergic activation in the ventromedial hypothalamus. *Am J Physiol Regul Integr Comp Physiol*. 2011; 301:R1815–1820. [PubMed: 21957162]
34. Satoh N, et al. Sympathetic activation of leptin via the ventromedial hypothalamus: leptin-induced increase in catecholamine secretion. *Diabetes*. 1999; 48:1787–1793. [PubMed: 10480609]
35. Takaki A, Nagai K, Takaki S, Yanaihara N, Nakagawa H. Satiety function of neurons containing a CCK-like substance in the dorsal parabrachial nucleus. *Physiol Behav*. 1990; 48:865–871. [PubMed: 2087519]
36. Yoshimatsu H, Egawa M, Bray GA. Effects of cholecystokinin on sympathetic activity to interscapular brown adipose tissue. *Brain Res*. 1992; 597:298–303. [PubMed: 1473000]
37. Le Lay J, et al. CRTC2 (TORC2) contributes to the transcriptional response to fasting in the liver but is not required for the maintenance of glucose homeostasis. *Cell Metab*. 2009; 10:55–62. [PubMed: 19583954]
38. Krashes MJ, et al. Rapid, reversible activation of AgRP neurons drives feeding behavior in mice. *The Journal of clinical investigation*. 2011; 121:1424–1428. [PubMed: 21364278]
39. Armbruster BN, Li X, Pausch MH, Herlitze S, Roth BL. Evolving the lock to fit the key to create a family of G protein-coupled receptors potentially activated by an inert ligand. *Proc Natl Acad Sci U S A*. 2007; 104:5163–5168. [PubMed: 17360345]

40. Wu Q, Clark MS, Palmiter RD. Deciphering a neuronal circuit that mediates appetite. *Nature*. 2012; 483:594–597. [PubMed: 22419158]
41. Leininger GM, et al. Leptin action via neurotensin neurons controls orexin, the mesolimbic dopamine system and energy balance. *Cell Metab*. 2011; 14:313–323. [PubMed: 21907138]
42. Leshan RL, Greenwald-Yarnell M, Patterson CM, Gonzalez IE, Myers MG Jr. Leptin action through hypothalamic nitric oxide synthase-1-expressing neurons controls energy balance. *Nat Med*. 2012; 18:820–823. [PubMed: 22522563]
43. Song P, Mabrouk OS, Hershey ND, Kennedy RT. In vivo neurochemical monitoring using benzoyl chloride derivatization and liquid chromatography-mass spectrometry. *Anal Chem*. 2012; 84:412–419. [PubMed: 22118158]
44. Jiang L, He L, Fountoulakis M. Comparison of protein precipitation methods for sample preparation prior to proteomic analysis. *J Chromatogr A*. 2004; 1023:317–320. [PubMed: 14753699]
45. Kawamori D, et al. Insulin signaling in alpha cells modulates glucagon secretion in vivo. *Cell Metab*. 2009; 9:350–361. [PubMed: 19356716]
46. Jacobson L, Ansari T, McGuinness OP. Counterregulatory deficits occur within 24 h of a single hypoglycemic episode in conscious, unrestrained, chronically cannulated mice. *Am J Physiol Endocrinol Metab*. 2006; 290:E678–684. [PubMed: 16533951]

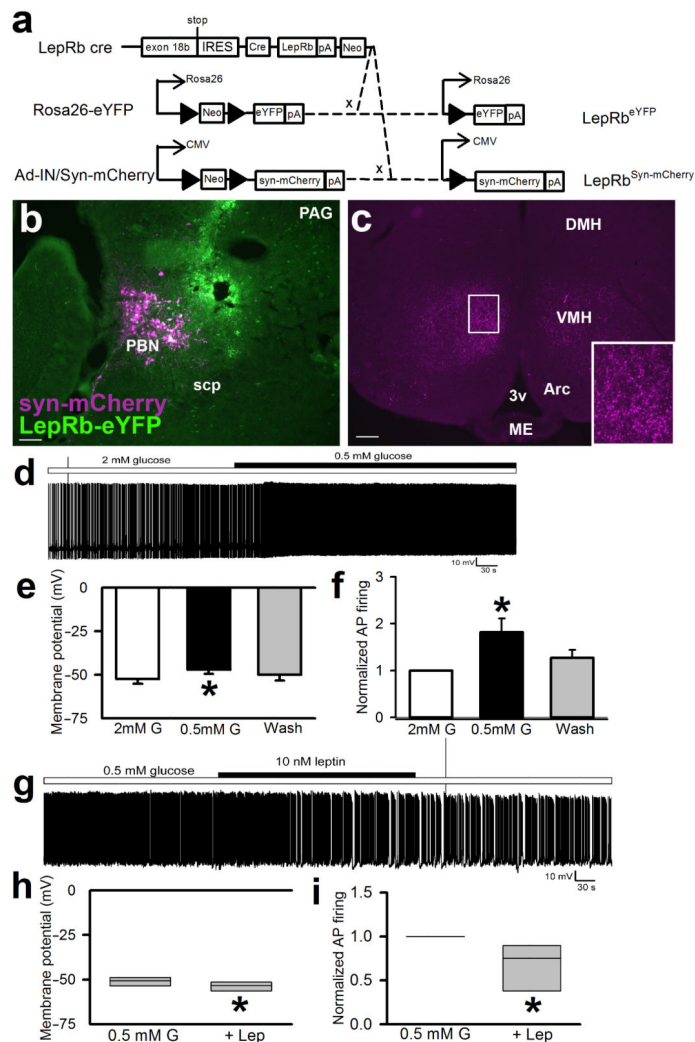


Figure 1. VMH-projecting PBN LepRb neurons are activated by low glucose and inhibited by leptin

(a) *Lepr^{cre}* mice were crossed onto the Rosa26-eYFP background to generate LepRb^{eYFP} mice expressing eYFP in LepRb neurons and/or were injected with the cre-inducible adenoviral tracing vector, Ad-iN/Syn-mCherry, to induce Syn-mCherry expression in LepRb neurons at the site of injection. (b, c) Ad-iN/Syn-mCherry was injected into the PBN of LepRb^{eYFP} mice. Mice were perfused and brain sections were stained for dsRed (syn-mCherry; purple) and/or GFP (eYFP; green). (b) Representative injection site in the PBN; (c) representative section showing the main projection target—the VMH. Scale bars= 100 μ m. Images shown are representative of injections in 8 separate animals. Inset—digital zoom of the indicated area. scp=superior cerebellar peduncle; 3v=third cerebral ventricle; ME=median eminence; Arc=arcuate nucleus; VMH=ventromedial hypothalamic nucleus; DMH=dorsomedial hypothalamic nucleus. (d-i) Fluorescently-detected PBN LepRb neurons in horizontal sections were studied for responses to glucose and leptin in current-clamp mode. (d) Representative trace of membrane potential at baseline in 2 mM glucose and following switch to 0.5 mM glucose. Membrane potential (e) $*p=0.01$, $\{F(2,14)=7.659\}$ and

action potential (AP) frequency (f) were measured $*p=0.042$, $\{F(2,14)=4.012\}$; $N=6$ individual neurons from four different animals. (g) Representative trace of membrane potential recorded in 0.5 mM glucose and in 0.5 mM glucose with the addition of leptin (10nM). Membrane potential (h) $*p=0.011$ $\{t(5)=3.94\}$ and AP frequency (i) $*p=0.037$ $\{t(5)=2.83\}$ were measured; $N=6$ individual neurons from four different animals. Data in e-f were analyzed by one way repeated measures ANOVA; data in h-i were analyzed by paired two tailed t-test. Data plotted as mean \pm SEM (e-f). Data plotted as Q1, Q2, and Q3 (h-i).

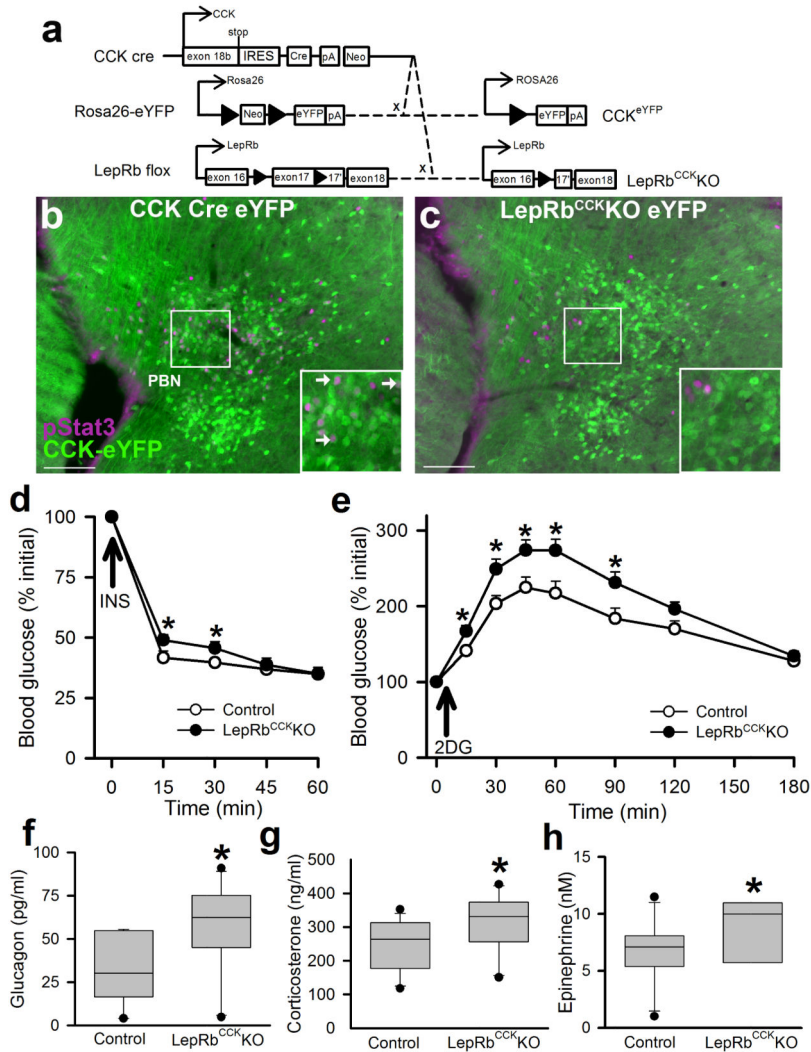


Figure 2. Deletion of LepRb from PBN CCK cells blunts IIH and augments the CRR to glucoprivation

(a) *Cck^{cre}* mice were crossed onto the Rosa26-eYFP background to generate CCK^{eYFP} mice expressing eYFP in CCK neurons and/or were crossed onto the *LepR^{flox}* background to generate *LepRb^{CckKO}* mice. (b, c) CCK^{eYFP} (b) and *LepRb^{CckKO}*eYFP (c) mice were injected with IP leptin (5 mg/kg) 2 hours prior to perfusion and immunostaining for pSTAT3 (purple) and GFP (eYFP; green). The PBN of representative mice is shown; representative of at least 3 mice per genotype. Scale bars= 100 μ m. Inset-digital zoom of the indicated area; arrowheads indicate colocalized neurons. (d) Hypoglycemic response to IP insulin administration (1 U/kg) in male *LepRb^{CckKO}* mice or control genotype littermates. N=11 (con) and 12 (ko) animals; p=0.01 (15min),0.03 (30min){F(4,21)=2.55} test; all data are plotted as mean \pm SEM. (e-h) Male Control and *LepRb^{CckKO}* mice were injected with 2DG (250 mg/kg, IP) and monitored for 180 minutes. (e) Blood glucose was monitored at the indicated times; *p=0.004 (30min),0.002 (45min),<0.001 (60min),0.003 (90min) {F(7,22)=3.3}, N= 11 (con) and 13 (ko) animals. Plasma glucagon (f) *p=0.008 {t(20)=-2.641}, N=11 animals per condition, corticosterone (g) p=0.029 {t(20)=-2.01},

N=11 animals per condition, and epinephrine (h) * $p=0.044$ { $t(17)=-1.80$ }, N=11 (con) and 8 (ko) animals, 90 minutes after 2DG administration. Panels d-h: n=8-12 animals per condition, representative of 6 similar experiments; data are plotted as mean \pm SEM (d-e) or Q1, Q2, and Q3 with 10th and 90th percentiles as whiskers (f-h)..* $p<0.05$ d and e were analyzed by two way repeated measures ANOVA with Fisher LSD post hoc test. Hormone levels (f-h) were analyzed by one tailed t-test, consistent with our directional hypothesis.

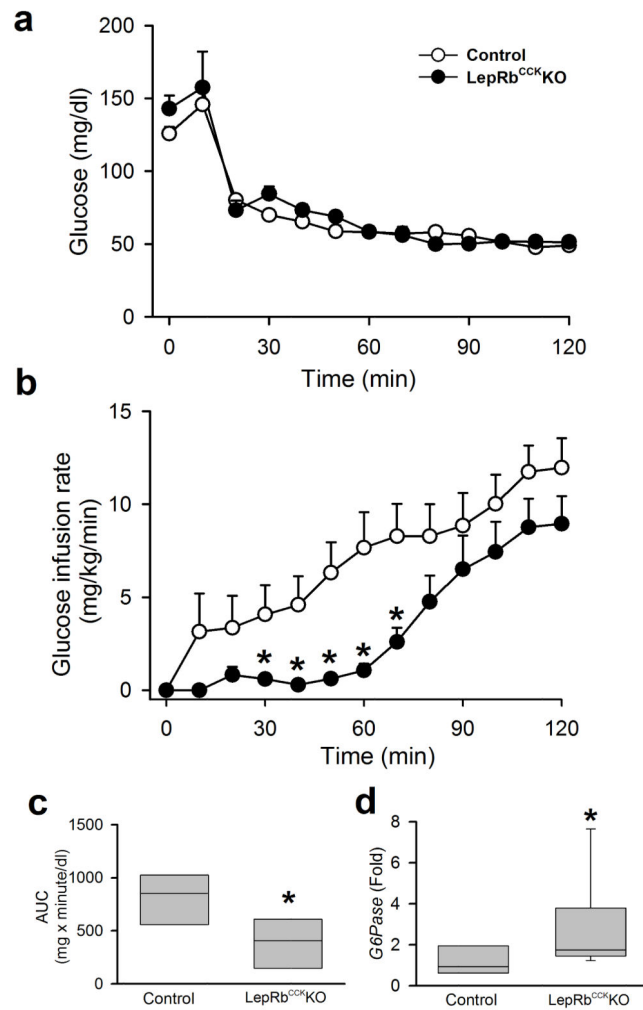


Figure 3. Enhanced CRR during hypoglycemic clamp in *LepRb^{Cck}KO* mice

Male *LepRb^{Cck}KO* mice or littermates of control genotypes with arterial catheters were infused with insulin to suppress blood glucose and activate the CRR. For the subsequent 120 minutes, (a) blood glucose was monitored and glucose infusion rate (b) was adjusted to maintain blood glucose at approximately 50 mg/dl; * $p=0.004$ (30min), 0.002 (40min), <0.001 (50min), <0.001 (60min), 0.002 (70min) { $F(12,13)=2.70$ }, $N=7$ (con) and 8 (ko) animals. (c) Area under the curve (AUC) for the data graphed in (b) * $p=0.014$, { $t(13)=2.84$ } $N=7$ (con) and 8 (ko) animals. (d) hepatic *G6Pase* mRNA expression (fold over control) at the end of the clamp * $p=0.015$, { $t(14)=-2.41$ }, $N=7$ (con) and 9 (ko) animals. data in a-b are plotted as mean \pm SEM and as Q1, Q2, and Q3 with whiskers at the 10th and 90th percentiles in c-d. Data in b were analyzed by two way repeated measures ANOVA with Fisher LSD post hoc test; c-d were analyzed by one tailed t-test, consistent with our directional hypothesis.

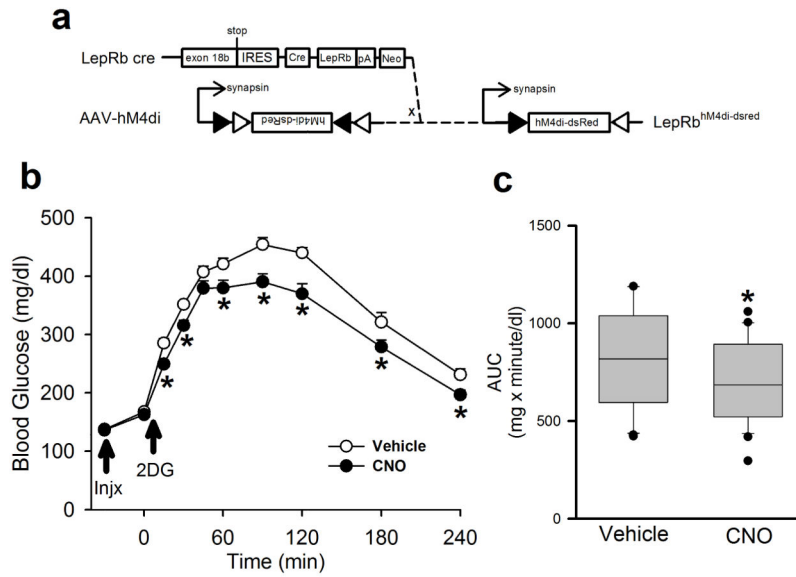


Figure 4. Inhibition of PBN LepRb neurons blunts the hyperglycemic response to glucoprivation (a) Bilateral injection of the cre-inducible AAV-hM4Di into the PBN of male *LepR^{cre}* mice induces the expression of the inhibitory DREADD hM4Di in PBN LepRb neurons. Animals were injected with Vehicle or CNO (Injx: 0.3 mg/kg, IP) and then with 2DG (250 mg/kg, IP) and blood glucose was monitored for 240 minutes. (b) Blood glucose was monitored at the indicated times; *p=0.005 (15min), 0.017 (30min), 0.021 (60min), <0.001 (90min), <0.001 (120min), 0.004 (180min), <0.001 (240min) {F(9,38)=1.91} N=20 (veh) and 20 (cno) animals. (c) Area under the curve (AUC) for the data graphed in (b); p<0.001 {t(38)=4.22} N=20 (veh) and 20 (cno) animals. all data are plotted as mean +/- SEM. The data in b were analyzed by two way repeated measures ANOVA with Fisher LSD post hoc test; c was analyzed by two tailed t-test. Data in a is plotted as mean +/- SEM and as Q1, Q2, and Q3 with whiskers at the 10th and 90th percentiles in b.

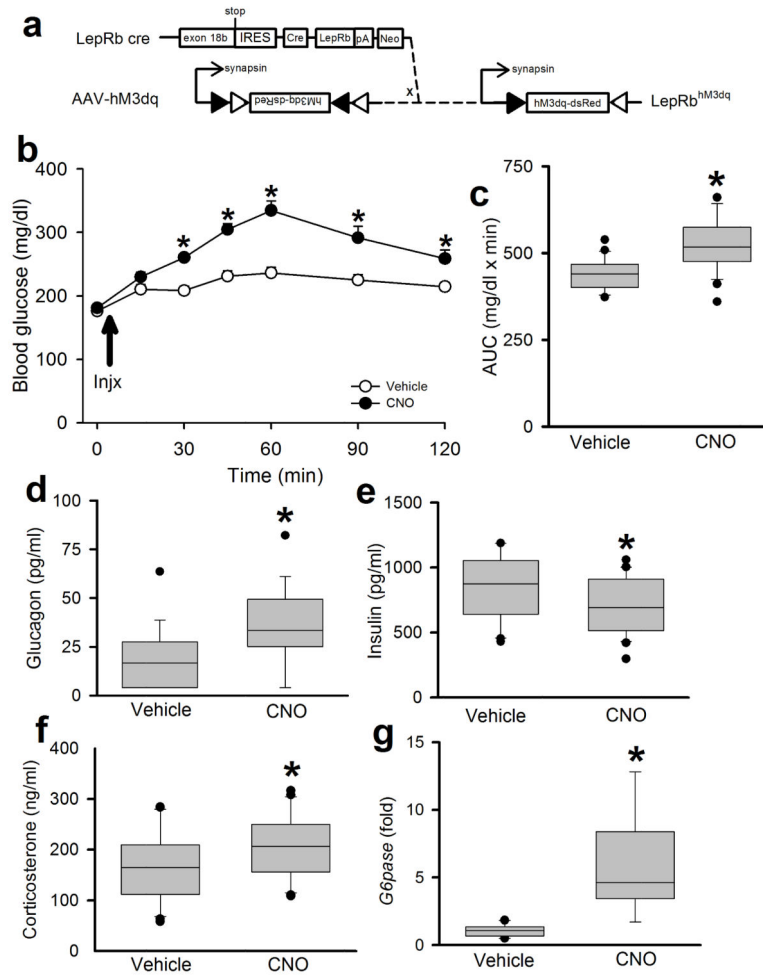


Figure 5. Activation of PBN LepRb neurons mimics the CRR to glucoprivation

(a) Bilateral injection of the cre-inducible AAV-hM3Dq into the PBN of male *LepR^{cre}* mice induces the expression of the activating DREADD hM3Dq in PBN LepRb neurons. Animals were injected with Vehicle or CNO (0.3 mg/kg, IP) and monitored for 120 minutes. (b) Blood glucose was monitored at the indicated times *p<0.001 (15min), <0.001 (30min), <0.001 (45min), <0.001 (60min), <0.001 (90min), 0.002 (120min) {F(6,30)=8.23}, N=16(veh) and 16(cno) animals. (c) Area under the curve (AUC) for the data graphed in (b); *p<0.001 {t(42)=-4.38} N=22 (veh) and 22 (cno) animals. Plasma glucagon (d) *p=0.002 {t(35)=-3.03} N=18(veh) and 19(cno) animals, insulin (e) *p=0.049 {t(40)=1.69} N=21(veh) and 21(cno) animals, corticosterone (f) 30 minutes after CNO administration *p=0.034 {t(40)=-1.87}, N=21(veh) and 21 (cno) animals. (g) hepatic *G6Pase* mRNA expression (fold over control) at the end of the experiment *p<0.001 {t(17)=-6.64}, N=10 (veh) and 9 (cno) animals. all data are plotted as mean \pm SEM. *p<0.05 The data in b were analyzed by two way repeated measures ANOVA with Fisher LSD post hoc test. The data in c were analyzed by two tailed t-test; d-g were analyzed by one tailed t-test, due to our directional hypothesis. Data in b is plotted as mean \pm SEM and as Q1, Q2, and Q3 with whiskers at the 10th and 90th percentiles in c-g.

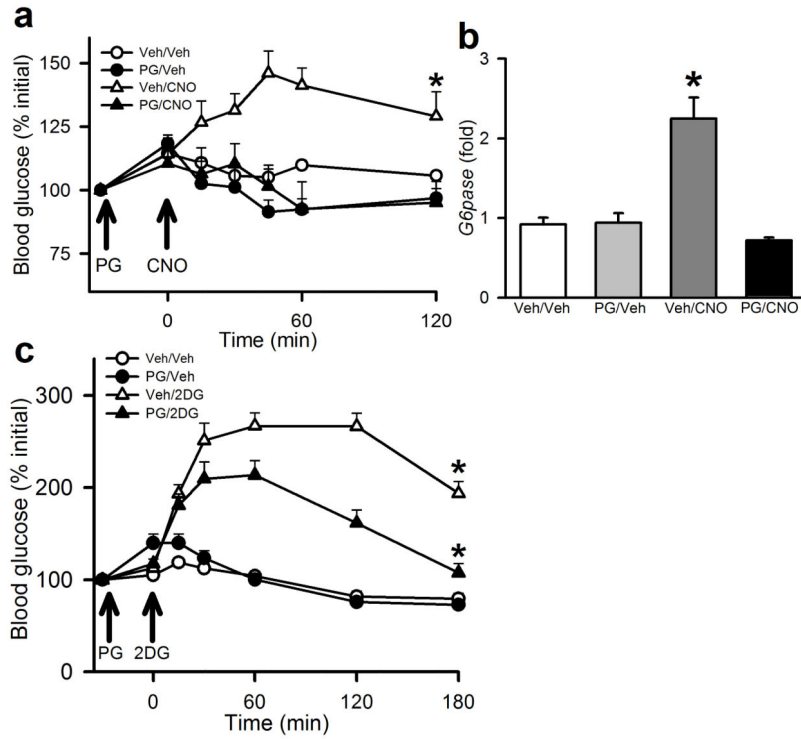


Figure 6. CCK-dependence of the hyperglycemic responses to activation of PBN LepRb neurons and glucoprivation

(a, b) Male *Lepr^{cre}* mice were injected bilaterally with the activating DREADD hM3D_q and allowed to recover for at least two weeks. Animals were injected with Proglumide (PG; 20 mg/kg, IP) or Vehicle (Veh) and 30 minutes later were injected with vehicle or CNO (0.3 mg/kg, IP) and (a) blood glucose was monitored at the indicated times; {F(3,16)=6.19}, N=3(v/v), 3 (pg/v), 7(v/c), and 7 (pg/c) animals. (b) Hepatic *G6Pase* mRNA expression (fold over control) was measured at the end of the experiment; p<0.001 from all groups {F(3,13)=21.839}, N=5 (v/v), 4 (pg/v), 4 (v/c), and 4 (pg/c) animals. All data are plotted as mean \pm SEM (c) C57Bl/6 mice were injected with Proglumide (PG; 100 mg/kg, IP) or Vehicle and 30 minutes later were injected with vehicle or 2DG (500 mg/kg, IP) and blood glucose was monitored at the indicated times; {F(3,25)=43.47}, N=6 (v/v), 7 (pg/v), 8 (v/2dg), and 8 (pg/2dg) animals. All data are plotted as mean \pm SEM. The data included in panels a and c were analyzed by two way repeated measures ANOVA with Fisher LSD post hoc test; the data in panel b was analyzed by one way ANOVA with Fisher LSD post hoc test. A:*p=0.006 vs(PG/Veh), 0.001 vs (PG/CNO), and 0.031 vs (Veh/Veh). C:*p<0.001 vs all groups.